Supplementary methods

Southern blot analysis for the *chFP* transgene

Genomic DNA (5 µg/lane) was electrophoresed in a 0.8% agarose/Tris acetate (TAE) gel at 46 V for 5 h. Gels were then denatured for 30 min at room temperature in 0.5 M NaOH, 1.5 M NaCl, neutralized for 30 min in 0.5 M Tris-HCl (pH 7.0), rinsed for 30 min in 20× SSC then transferred to a nylon membrane (Hybond, Amersham) overnight at room temperature. The blot was rinsed in 2× SSC, allowed to dry on 3 mm filter paper, cross-linked (Stratagene) and stored dry between sheets of 3 mm filter paper until used. A 646 bp probe against the Woodchuck hepatitis virus promoter response element (WPRE) region of the transgene was generated by cutting the pLenti.PGK1:eGFP lentivector with *Bgl*II and *Sal*I, gel isolating the linearized fragment, and labeling it with ^{32}P dCTP (Perkin Elmer) using a random priming kit (RediPrime II, Amersham, GE Healthcare), and hybridized. Blots were imaged using a Storm 840 phosphorimager (Molecular Dynamics).

Cell proliferation assay

The Click-iT EdU assay (Invitrogen) was used to assay *in vivo* cell proliferation according to manufacturers recommendations. The EdU assay uses a copper catalyzed cycloaddition reaction between the terminal alkyne group of the thymine analog EdU (5'-ethynyl-2'-deoxyuridine) and a fluorophore-conjugated azide molecule. The EdU assay (Warren et al., 2009) was carried out on cultured quail embryo. EdU (Click-iT EdU kit, Cat. #C10083 Invitrogen) was diluted in PBS at 10 mM (stock solution). 50 µl of working dilution (500 µM) was dropped on embryos incubated for 40 h (developmental stages 7-10), which were incubated for 6 h. The embryos were washed with PBS and fixed in 4% formaldehyde [36% formaldehyde (47608, Sigma) diluted to 4% in PBS]. The percentage of EdU-positive cells and level of chFP signals were quantified using the spot function of Imaris (Bitplane) software. Between 72 and 643 cells were analyzed for each embryonic territory. The linear correlation is significant at a level of 0.05. The standard error of the slope was found from the sum of squared differences of x and y for the five data points and used to calculate a t statistic of –3.36. For a two-tailed test, this t statistic correlates to a P-value of 0.044 at three degrees of freedom. Standard error of the mean was computed and is represented as error bars.

Microscopy

For static whole-mount images, the embryos were isolated from the yolk using paper rings, washed in PBS, fixed in 4% paraformaldehyde/PBS at 4ºC for 16 hours, washed again in PBS, and stained with DAPI (0.5 µg/µl) for 2 h at room temperature. Embryos were then washed in PBS and mounted between two #1 coverslips using Permafluor mounting media (Thermo Scientific) and stored in the dark at 4ºC until imaging. For vibratome sectioning, the chFP$^+$ DAPI-stained embryos were embedded in a warm mixture of 3% agarose and acrylamide/bis-acrylamide/TEMED (Germroth et al., 1995). Cross-linking was initiated by the addition of 0.1% ammonium persulfate while on ice. The resulting blocks were serially cross-sectioned at 70 µm on a Leica 1200 vibratome. For dynamic images, embryos were isolated from the yolk using a modified paper ring EC (Early Chick) culture system (Chapman et al., 2001). Briefly, a thin bed of agar/albumin was poured into several 35 mm culture dishes and a single two-well Lab Tek chambered #1 coverglass slide (Thermo Scientific) and allowed to solidify. After removal from the yolk, the embryos were briefly washed in sterile PBS and placed dorsal side down on the agar/albumin bed in the 35 mm Petri dishes. The embryos were returned to the 37ºC incubator for 2 h to recover then screened under an Olympus MVX10 stereomicroscope for the presence of the fluorescent reporter and normal morphology. Selected embryos were transferred dorsal side down onto the agar bed of the two chamber imaging slide and the lid was sealed with parafilm. The slide was mounted onto the stage of the confocal microscope which had been pre-warmed to 37ºC using an electronically controlled environmental chamber (Pecon). The embryo was incubated on the microscope for 2 h to allow the embryo to settle down into the agar/albumin layer before imaging was initiated.

3D imaging metadata for various developmental stages
Microscope metadata: Zeiss LSM 780 (inverted) equipped with 34 channel GaAsp Spectral Detectors, 5 laser lines (405, 458, 488, 514, 561 and 633 nm), and run with ZEN 2011 system software was used to collect all the 3D images of various developmental stages.
Microscope metadata: Zeiss LSM 780 inverted confocal microscope; Plan-Apochromat 20x/0.8 WD=0.55 M27 objective; Ex 405 (1.2%)/Em 409-584; Ex 561 (5.0%)/Em 571-695; Pixel dwell time, 12.6 µsec; mean of 2 line scans.

Additional metadata for each collection is detailed below:

Developmental stage X (Fig. 1B,C)
Dimensions: 5020.62 x 5062.96 x 35.00 μm^3 (16 *z*-sections); Resolution: 1.20 pixels per µm; Voxel size: 0.83 x 0.83 x 2.5 μm^3; Bits per pixel: 16.

Developmental stage 11 (Fig. 1D,E)
Dimensions: 1208.04 x 5426.62 x 244.0 μm^3 (61 *z*-sections); Resolution: 1.20 pixels per µm; Voxel size: 0.83 x 0.83 x 4 μm^3; Bits per pixel: 16.

3D imaging by two-photon microscopy (Fig. S6)
A fixed stage 10 Tg(PGK1:H2B-chFP) embryo was mounted in glycerol.
Microscope metadata: Zeiss LSM 780 inverted confocal microscope powered by a Titanium:Sapphire (Ti:Sa) laser (810 nm pump) coupled to an OPO system (Coherent); C-Achroplan 32x/0.85 W Corr M27 objective (Zeiss); Ex 1050 (50%); main beam splitter MBS 690+ was used as well as BS-MP-760. zoom was set up at 0.6; pixel dwell time, 25.2 µsec; mean of 2 line scans; master gain was set up at 812. The NDD external detector BIG (Zeiss) was used to collect the signal.

4D imaging metadata for various time-lapse experiments
For dynamic imaging we used whole-mount *ex ovo* avian embryo culture previously described (Drake et al., 1992; New, 1955; Sato et al., 2010). A Zeiss LSM 510 META inverted confocal microscope equipped with an onstage incubator maintained the temperature at 36ºC during imaging was used to acquire Movies 1-2 and 4-10.

Multicolor mosaic stitching
Mosaic stitching was performed using Zeiss Zen, or Fiji after color-balance correction. *xy* translation between images was evaluated using single *z*-slices, or maximum-intensity projections when possible.

Image analysis
Image analysis was performed using ImageJ (US National Institutes of Health), Fiji (http://fiji.sc/), MATLAB (MathWorks) and Imaris (Bitplane). Since all cells in the Tg(PGK1:H2B-chFP) quail contain a detectable fluorescent label, the number of cells to be followed is large (hundreds to thousands), requiring 'multiple-particle tracking.' Cell behaviors were analyzed using Imaris (Bitplane), Fiji and MATLAB software. LSM formatted images classified into image sets were processed using various image analysis tools/algorithms. The data output from the image analysis pipeline is a set of cell parameters and images for visual inspection. Information from tracked cells was extracted from processed image sets for further data analysis. Typical parameters obtained from each image set include nuclear perimeter, volume and mean pixel intensity. Other measurements first require the identification of individual cells across multiple frames in order to determine parameters of cell motility (e.g. velocity, direction, persistence), rates and orientations of cell division, and daughter cell and tissue-specific cell movements. The data extracted from image sets are saved as a set of Excel files for statistical analysis.

All images were stored in the original .lsm format and copies were manipulated using Photoshop CC (Adobe) and movies were annotated in Premiere Pro CC (Adobe). All original high-resolution image sets are available upon request.

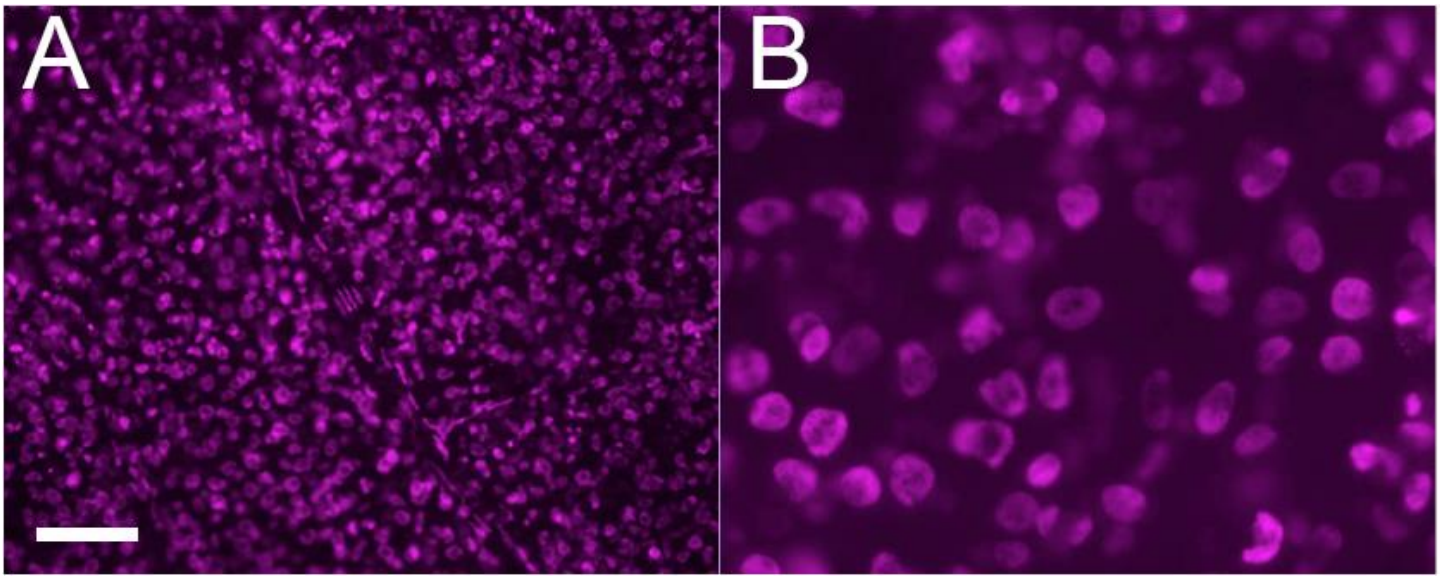

Fig.S1. Fluorescent stereomicroscope image of the CAM inside a newly hatched Tg(PGK1:H2B-chFP) egg. (A) Fluorescence dissecting microscope acquired image of H2B-chFP+ calls that comprise the CAM within the shell from the offspring of a Tg(PGK1:H2B-chFP) founder quail. (B) Same CAM as in (A) at 5X higher magnification showing cell nuclei expressing H2B-chFP. Scale bar, 20 um for A and 100 um for B.

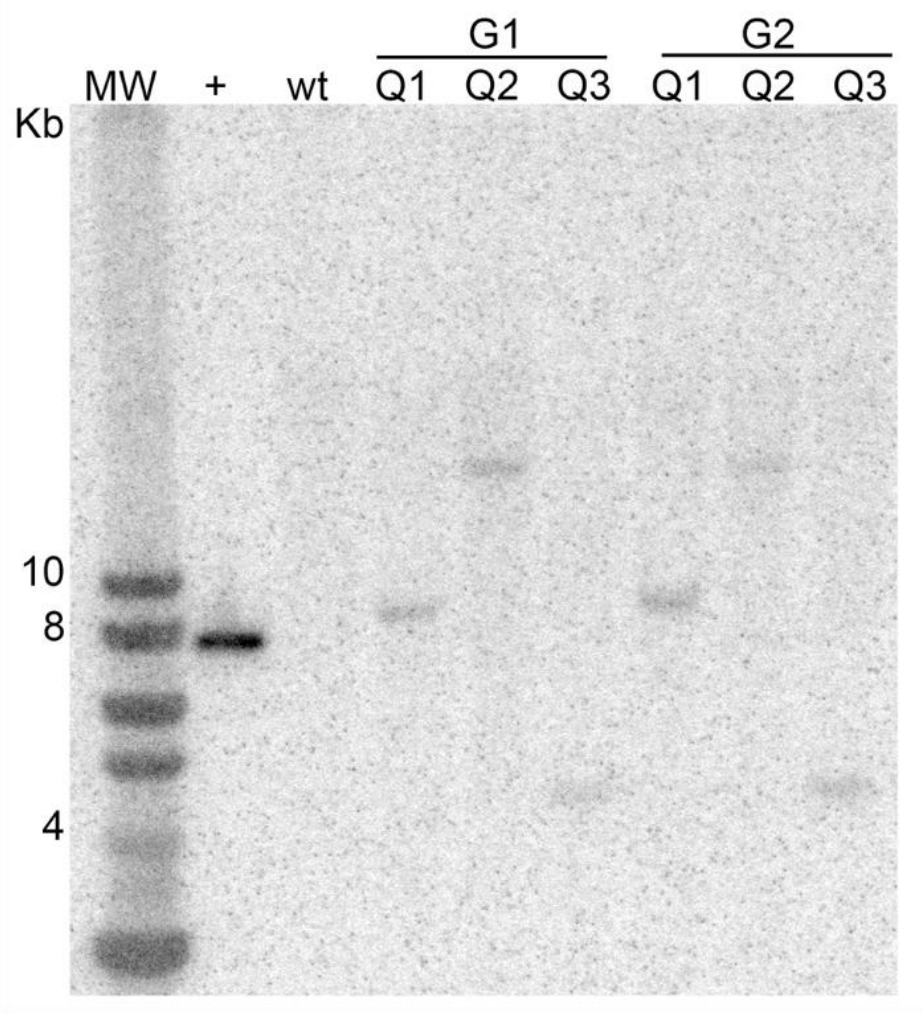

Fig.S2. Screening hatchling genomic DNA by Southern blot analysis.

Southern blot analysis of genomic DNA isolated from the chorioallantoic membrane of the eggshell from 3 different chimeric founders (G0). The gDNA was digested with Spe1, which cuts once inside the transgene, separated by gel electrophoresis and transferred to a nylon membrane. The blot was hybridized with a 646bp 32P-labeled probe designed to hybridize with the WPRE element within the transgene (Fig.1A). Three transgenic lines with single transgene integrations at distinct locations were identified and labeled as Q1 (9kb), Q2 (>10kb) and Q3 (5kb). When bred to a WT, these first generation (G1) birds produced genotypically positive second generation (G2) hatchlings as expected. + lane is the pPGK1:H2B-chFP lentivector shown in Fig.1A. WT lane is gDNA from a non-transgenic hatchling. MW lane is molecular weight markers in kilobases.

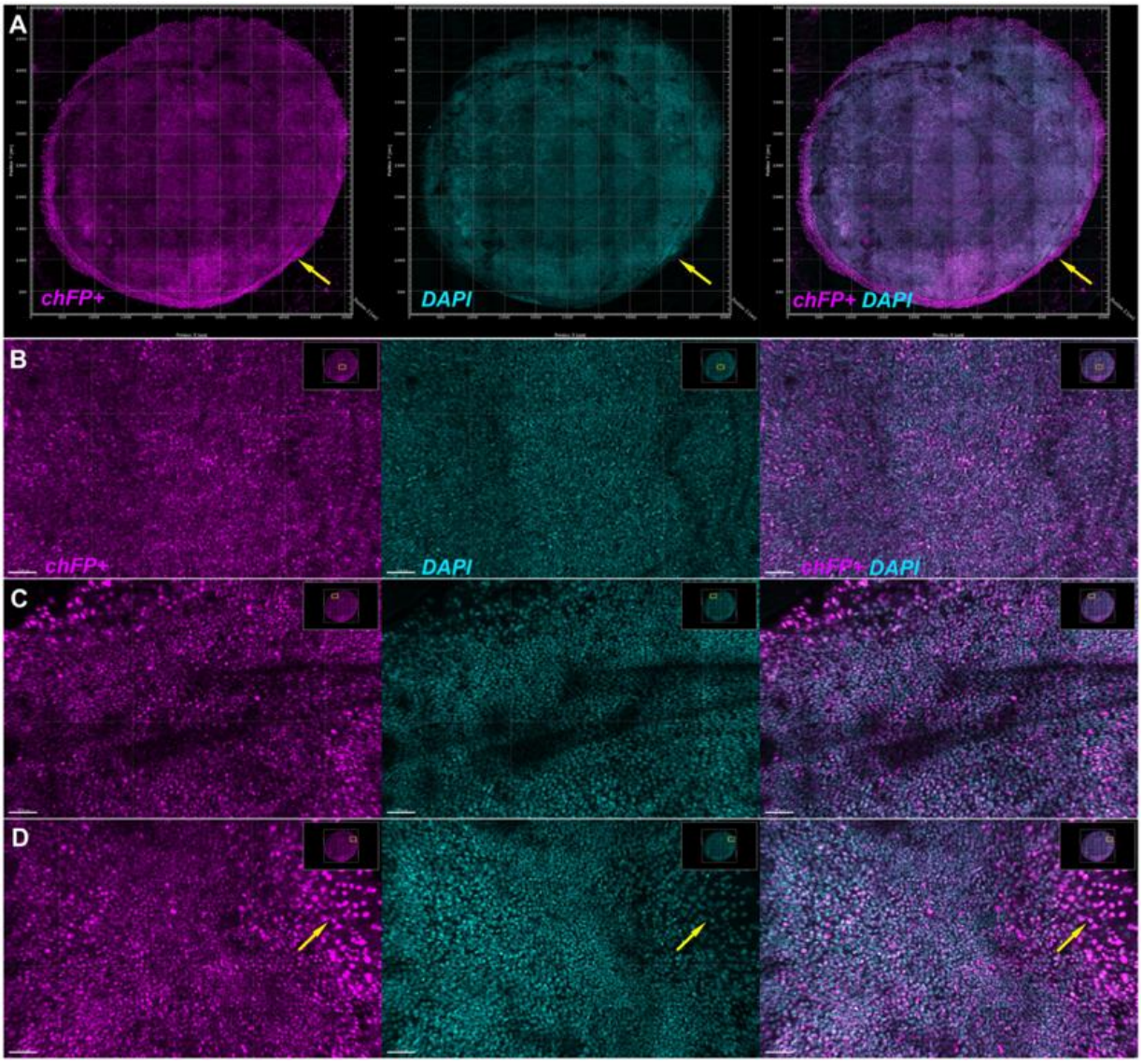

Fig.S3. Ubiquitous expression of PGK1:H2B-chFP transgene in developmental stage 2 embryos.

(A) Confocal microscope acquired images for chFP$^+$, DAPI, and chFP$^+$/DAPI overlay of a developmental stage 2 Tg(PGK1:H2B-chFP) quail embryo. Tg(PGK1:H2B-chFP) embryos ubiquitously express H2B-chFP during developmental stage 2. Note that the DAPI and chFP$^+$ relative fluorescence intensities do not always correlate, which is best discerned in the chFP$^+$/DAPI overlays. Putative hypoblast cells located at the posterior end of the embryo (A) and extra embryonic germ wall cells consistently display very high levels of chFP fluorescence (marked by yellow arrows in A, D). The relative chFP fluorescence intensity of these cells is 4-8-fold higher than the vast majority of the embryonic and extra embryonic cells (data not shown). (B-D) higher magnification images to confirm ubiquitous and heterogenous chFP+ expression. The precise location of the magnified images in terms of the entire stage 2 embryo can be seen in the upper right corner of each image. Dorsal view; anterior at top for all images. A) Grid scale marked every 500 um along xy axes; B-D) Lower left scale bar: 70 um. Dimensions: 5232.06 x 5244.51 x 92.0 μm^3 (23 *z*-sections); Resolution: 0.72 pixels per μm; Voxel size: 1.38 x 1.38 x 4 μm^3; Bits per pixel: 16.

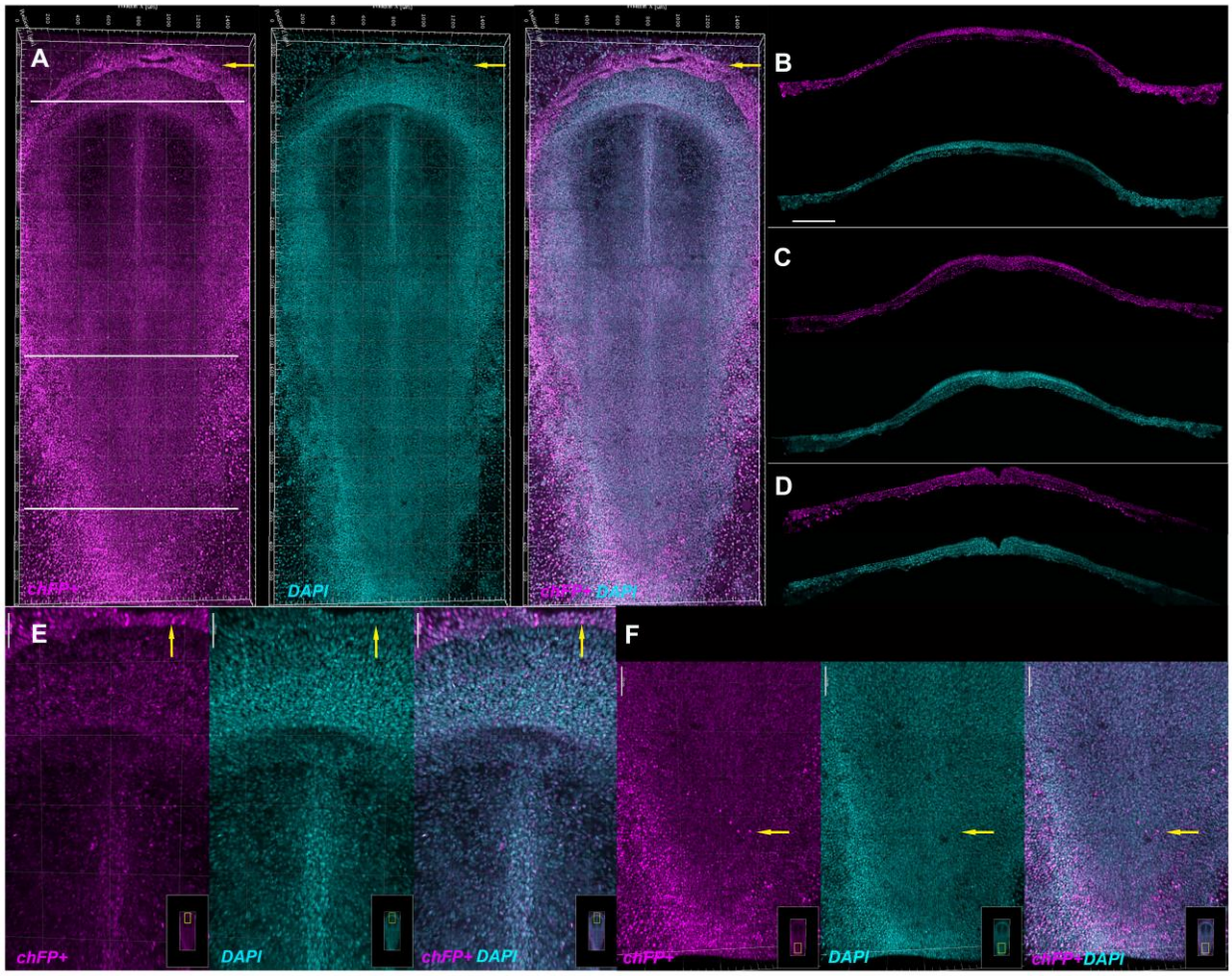

Fig.S4. Ubiquitous expression of PGK1:H2B-chFP transgene in developmental stage 5 embryos.

(A) Confocal microscope acquired images for chFP$^+$, DAPI, and chFP$^+$/DAPI overlay of a developmental stage 5 Tg(PGK1:H2B-chFP) quail embryo and (E-F) higher magnification images to confirm ubiquitous and heterogenous chFP$^+$ expression. Note that the DAPI and chFP$^+$ relative fluorescence intensities do not always correlate, which is best discerned in the chFP$^+$/DAPI overlays. Some extra embryonic (A, E, and F) and embryonic (A and F) cells display very high levels of chFP fluorescence (marked by yellow arrows). (B-D) Embryos were vibratome sectioned to generate transverse sections at approximately the A-P region noted by the white lines in A and imaged by confocal microscopy to confirm ubiquitous and heterogenous chFP$^+$ expression. Dorsal view; anterior at top for all images. A) Grid scale marked every 200 um along *xy* axes; B-D) scale bar: 200um; E-F) Vertical upper left scale bar: 100 um.

Dimensions: 1584.98 x 3860.74 x 148 µm^3 (37 *z*-sections); Resolution: 1.20 pixels per µm; Voxel size: 0.83 x 0.83 x 4 µm^3; Bits per pixel: 16.

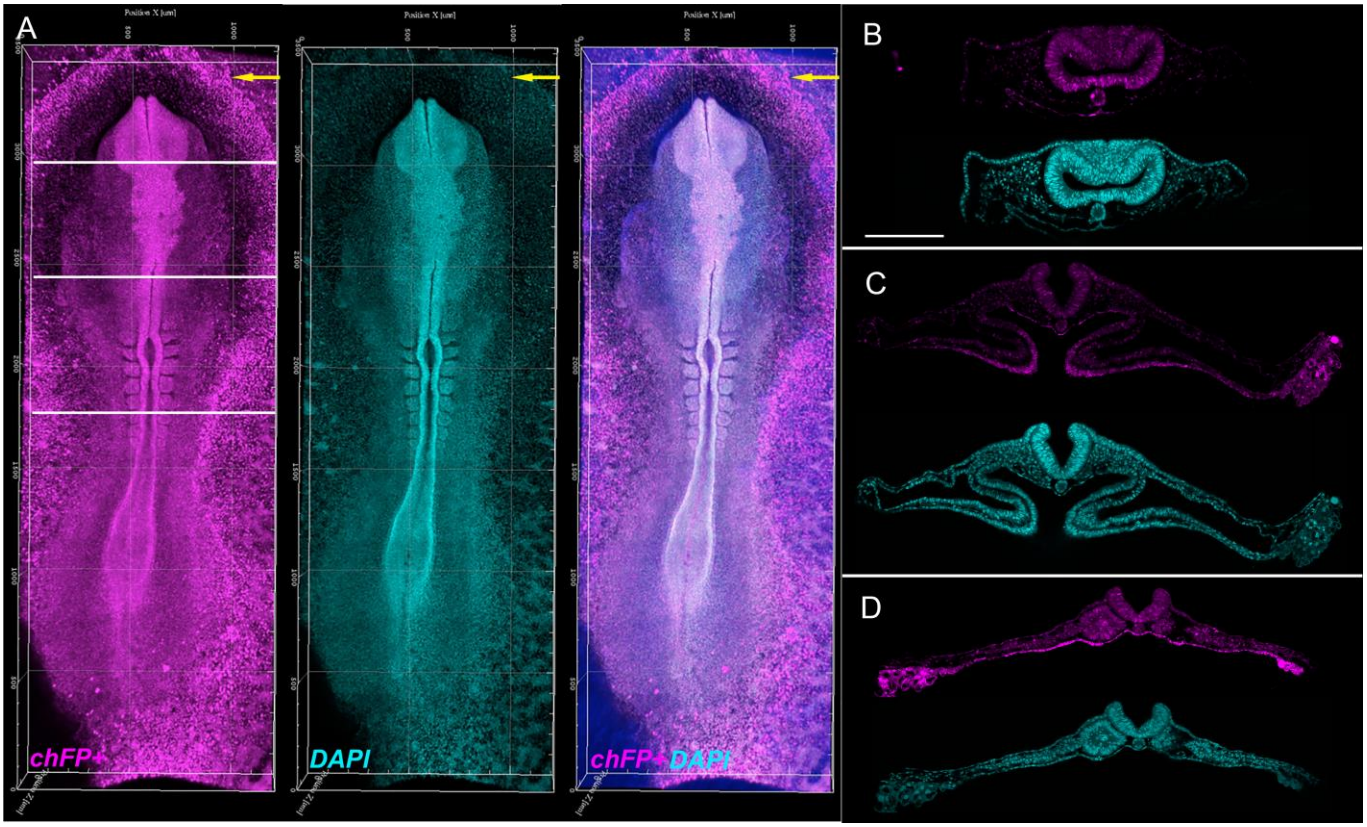

Fig.S5. Ubiquitous expression of PGK1:H2B-chFP transgene in developmental stage 9 embryos.

(A) Confocal microscope acquired images for chFP^{+}, DAPI, and chFP^{+}/DAPI overlay of a developmental stage 9 Tg(PGK1:H2B-chFP) quail embryo. (B-D) Embryos were vibratome sectioned to generate transverse sections at approximately the A-P region noted by the white lines in A and imaged by confocal microscopy to confirm ubiquitous and heterogeneous chFP^{+} expression. Dorsal view; anterior at top for all images. Dorsal view; anterior at top for all images. A) Grid scale marked every 500 um along xy axes. B-D) scale bar: 200um. Dimensions: 1210.53 x 3500.40 x 152 µm^3 (38 *z*-sections); Resolution: 1.20 pixels per µm; Voxel size: 0.83 x 0.83 x 4 µm^3; Bits per pixel: 16.

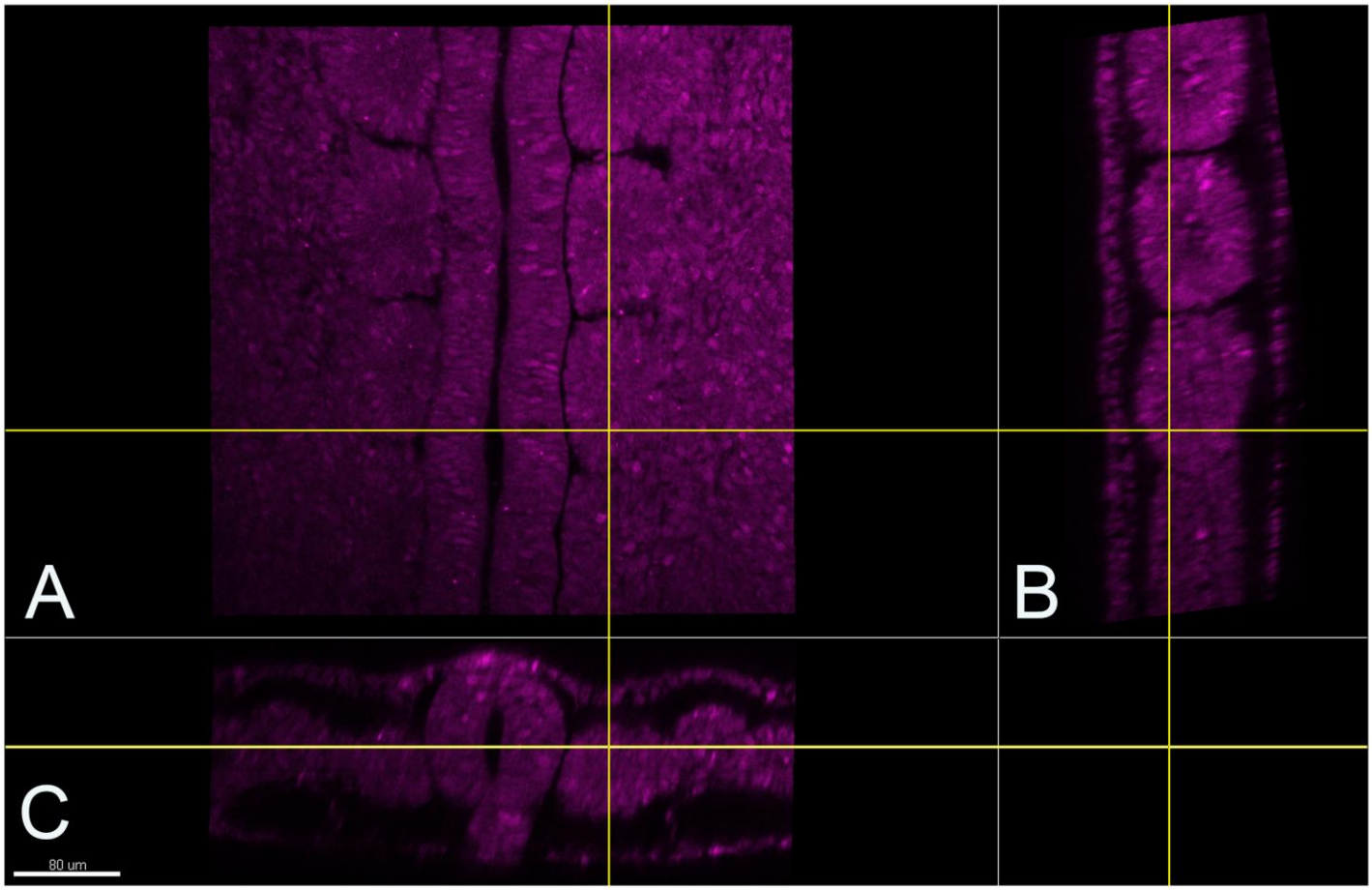

Fig. S6. 3D reconstruction of PGK1:H2B-chFP signal visualized by two-photon confocal microscopy.

3D reconstruction of PGK1:H2B-chFP signal in the trunk of a fixed stage 10 embryo visualized by 2 photon microscopy.(A) XY plane, (B) YZ plane, (C) XZ plane. Note that fluorescent signal can be detected throughout the embryo. Anterior is at the top in A and B. Dorsal is on the left in B. Ventral is on the bottom in C. Yellow lines demarcate the level at which planes are seen in neighboring panel. Image has been cropped using the crop 3D function of Imaris to remove regions without signal above and below the embryo. Scale bar for A-C is 80um.

Dimensions: 442 x 442 x 191 μm^3 (191 z-sections); Resolution: 0.865 pixels per µm; Voxel size: 0.865 x 0.865x 1 μm^3; Bits per pixel: 16.

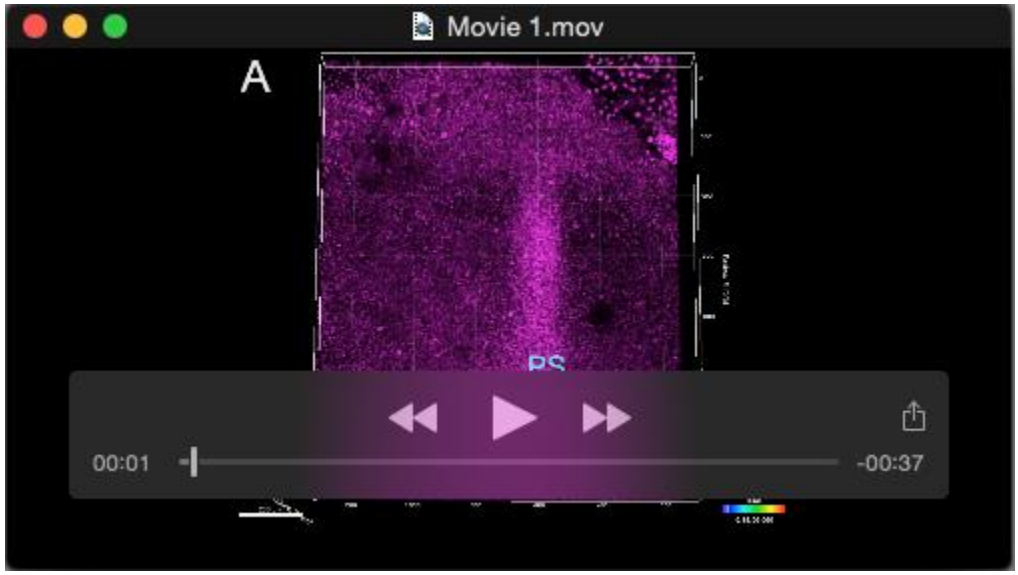

Movie 1. 4D imaging of gastrulating Tg(PGK1:H2B-chFP) embryo. 4D rendering of embryonic cells labeled with nuclear localized chFP and imaged by time-lapse confocal fluorescence microscopy over 86 time points at 15-min intervals for a total of 21:30 hrs. The embryo is oriented with the anterior end (A) on the left in order to view with higher resolution on a computer screen. The gastrulating embryo elongates along the A-P axis as converging epiblast cells intercalate along the midline to form the PS (~3:00:00 time point). The head fold process begins (~5:30:00) concomitant with continued A-P elongation. Somites 1 begin to form bilateral and adjacent to the PS (~8:30:00) and continue until the movie ends at the 8-somite stage (21:30:00). A-P elongation along the midline appears centered anterior to the future sites of somite 1 formation. Some extra embryonic within the area opaque consistently display very high levels of chFP fluorescence.

Ventral view. Lower left scale bar: 200 um; grid scale marked every 500 um along xy axes; time scale in lower right corner; A, anterior; D, dorsal; L, lateral; AO, area opaque; PS, primitive streak; HF, head fold. Lower right 3D arrows indicate that the embryo is oriented with anterior (A) to the left, lateral (L) to the bottom, and ventral (V) into the page.

Microscope metadata: Zeiss 510 META inverted, 20X/0.8 NA Plan-Apochromat; Ex 561 (15%)/Em LP 575.

Dimensions: 2812.51 x 1687.5 x 162 μm^3; Voxel size 2.2 x 2.2 x 6.0 μm^3.

Acquisition time: Image montage (5 x 3 x 22) at 15 min intervals per *xyz* tile for 86 time points (*t*) or 21:30:00 hrs was made by stitching *xyz* image sets across *t* with AIM LSM4.0 software.

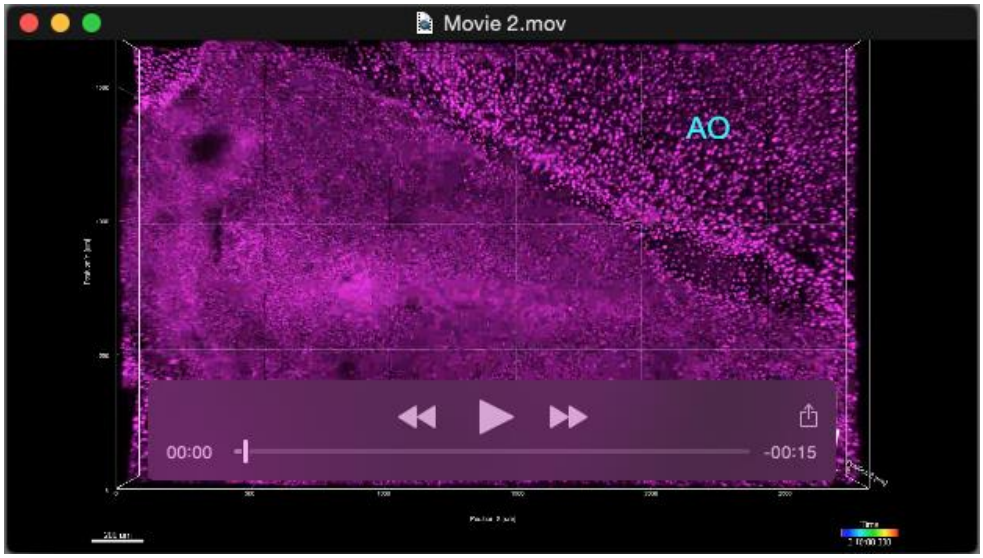

Movie 2. Cell and tissue movements during head fold process.

Compare with Movie 1 and Fig.3. Movie 2 derives from Movie 1, but was rotated 90 around the vertical axis and 180 around the horizontal axis for a preferred viewing perspective; the image set was also cropped initially in the *xy* dimensions and later in the *z* dimension in order to direct the attention of the reader and to reduce computational time. The embryo is oriented with the anterior end on the top.

(A) Maximum intensity projection of head fold process showing elongation along the A-P axis as converging epiblast cells intercalate along the midline thrusting the PS and adjacent tissue anterior until they fold ventrally and then descends in the posterior direction. As the ventral tissue moves posterior, adjacent lateral tissue simultaneously folds toward the midline to form the AIP.

(B) Tracking cells to show direction and speed of migration. The cell tracks are shown as white 'dragon tails' that represent a cell's location for the previous four time points (60 minutes) are overlayed on Movie 2A.

(C) The cell tracks are color coded 'dragon tails' that represent a cell's location and movement along the *y*-axis (-50 Anterior to 50 Posterior) for the previous four time points (60 minutes) are overlayed on Movie 2A.

(D) Tracking cells to indicate movement along the *y*-axis, direction, and speed of migration. The cell tracks are color-coded 'dragon tails' that represent a cell's location and movement along the *y*-axis (-50 Anterior to 50 Posterior) for the previous four time points (60 minutes).

(E) Movie 2A is re-oriented to better visualize the *z*-movements of cells and tissue. The anterior end is oriented into the screen and the central axis is tipped slightly to the right. This gives the viewer a perspective of looking into the forming AIP and permits the medio-lateral tissue movements to better visualized in 3D over time.

Ventral view. Lower left scale bar: 200 um; grid scale marked every 500 um along xy axes; time scale in lower right corner; Ant, anterior; AO, area opaque; PS, primitive streak; HF, head fold. Skewed perspective is 130% zoom. Lower left 3D arrows indicate that the embryo is oriented with anterior (A) to the top, lateral (L) to the left, and dorsal (D) into the page.

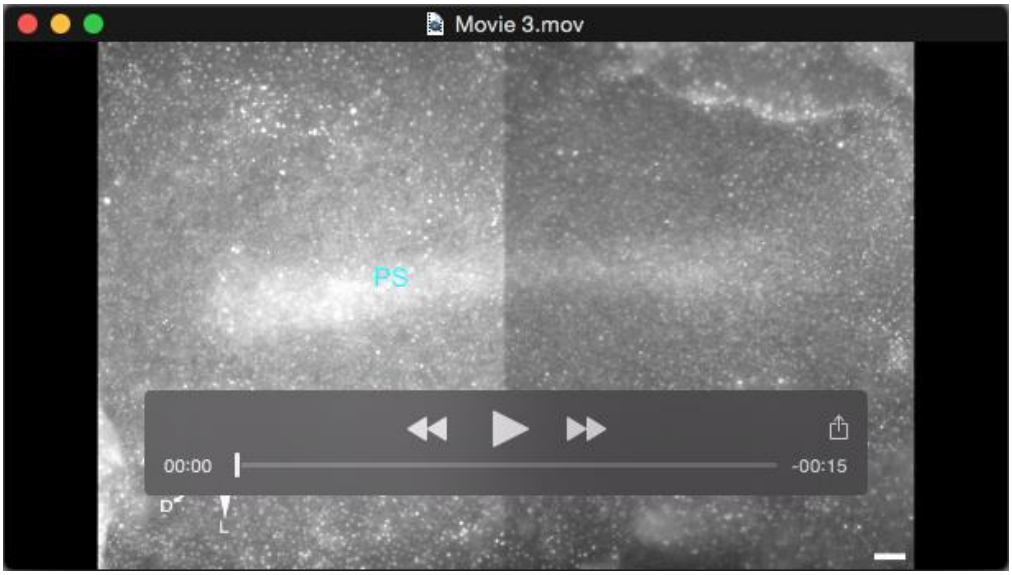

Movie 3. Wide-field fluorescence microscopy to evaluate large-scale tissue displacements.

Wide-field fluorescence microscopy of living Tg(PGK1:H2B-chFP) embryos captures the collective biological motion patterns that characterize early embryogenesis, including gastrulation, neurulation, somitogenesis, cardiogenesis, and neurogenesis recorded across 4 orders of spatial (400nm to 4 mm) and (1 minute to 1000 min) temporal resolution. The time-lapse sequence of Tg(PGK1:H2B-chFP) quail development begins during gastrulation and shows the movement of thousands of cells with the upper epiblast cells converging en masse toward the PS at the midline and cells of the bottom hypoblast layer moving radially outward and anterior (Frames 1-60). The PS extends anteriorly along the midline to orient the embryo along the A-P and D-V axes (Frames 1-75). As gastrulation proceeds, the A-P extension reaches a temporary maximum as the anterior head region folds back on itself, extends and moves posteriorly (Frame 75), A-P elongation continues and somites begin to form (Frame 83). As the head fold curves at the anterior end of the embryo, the tail folds at the posterior end, and then the lateral body folds at the sides of the embryo transforming the relatively flat gastrula into a three-dimensional organism. As AIP regression proceeds, the heart fields soon converge at the midline atop the regressing AIP, and assemble into the linear heart (H) tube by the end of the movie (Frame 140).

Ventral view. Scale bar in lower right corner represents 100 um; elapsed time and frame number are noted across the top of the movie; PS, primitive streak; HF, head fold; N, notochord; S, somite; AIP, anterior intestinal portal; Magenta asterisk (*) denotes approximate location of the regressing Hensen's node. Skewed perspective is 130% zoom. Lower left 3D arrows indicate that the embryo is oriented with anterior (A) to the left, lateral (L) to the bottom, and dorsal (D) into the page.

Microscope metadata: Brightfield and epifluorescence acquired on a Leica DM6000B upright microscope with the ventral side of the embryo facing the objective using a 5X/0.12P PL Fluotar objective, epifluroescence captured through Chroma mCherry/Texas Red filter set ET560/40ex ET630/75em with a T585lp beam splitter detected using a Retiga SRV deep cooled CCD camera. For each field and optical mode, images were acquired in 5 focal planes, so that the embryo remains in focus during extended recording times. The acquired images were processed to make full-scale images registered to correct for *xy* shifts during the experiment. (Czirok et al., 2002). The time-lapse movie was trimmed to 140 time points (20:40:35 hrs) in order to end at developmental stage 11.

Dimensions: 1796 x 2544 um^2; Pixel size 1.29 um^2 and the extended depth of field processed image encompassing 310 □m z resolution acquired and processed using KU TiLa acquisition and ImageJ for post processed image stack manipulations.

Acquisition time: Image montage (1 x 2 x 5) at ~10 min intervals per *xyz* tile as indicated by time stamps recorded at the initiation of each montage acquisition. Brightfield exposure times of 0.015 seconds and epifluroescent exposure times of 1.5 seconds were used.

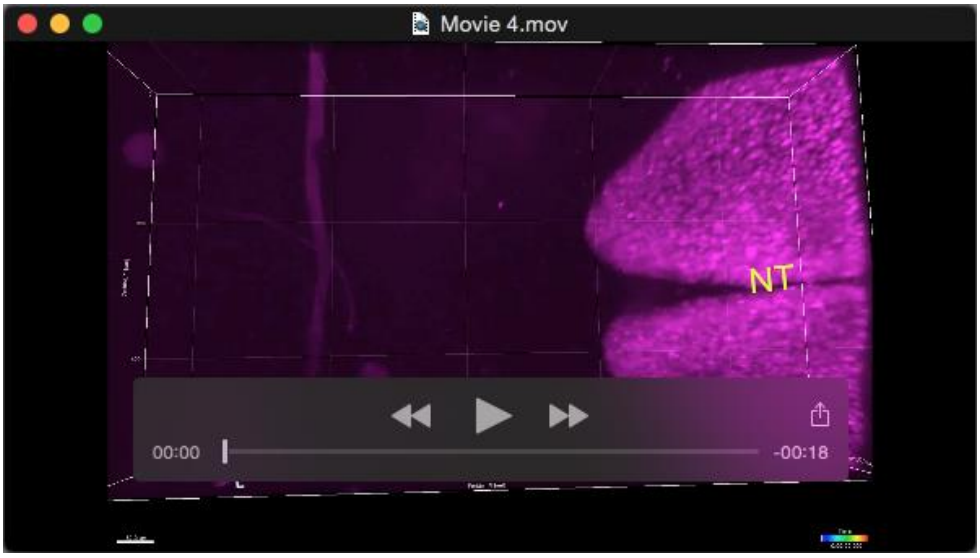

Movie 4. 4D imaging of cell movements during head formation using Tg(PGK1:H2B-chFP) embryo.

4D rendering of forming head region of Tg(PGK1:H2B-chFP) embryo over 107 time points at 5:10-min intervals. The anterior neuropore closes as NNE cells collectively move in anterior and ventral direction until frame 17, when the anterior edge of the embryo is at the 800 um X grid. The embryo elongates to the left as the NT elongates until frame 40, when the anterior edge of the embryo is at the 400 um X grid. As the anterior movement subsides, NC cells begin to delaminate from the NT and migrate bilaterally and ventrally along the inner side of the non-neural ectoderm (marked by cyan arrows).

Dorsal view. Lower left scale bar: 200 um; grid scale marked every 200 um along xy axes; time scale in lower right corner; A, anterior; NT, neural tube; NC, neural crest. Lower left 3D arrows indicate that the embryo is oriented with anterior (A) to the left, lateral (L) to the bottom, and ventral (V) into the page.

Microscope metadata: Zeiss 510 META inverted; 20X/0.8 NA Plan-Apochromat; Ex 561 (15%)/Em LP 575.

Dimensions: 1125.0 x 562.5 x 228 μm^3; Voxel size: 1.1 x 1.1 x 6.0 μm^3.

Acquisition time: Image montage (2 x 1 x 38) at 5:10 min intervals per *xyz* for a total of 10 hours, was made by stitching *xyz* image sets across *t* with AIM LSM4.0 software.

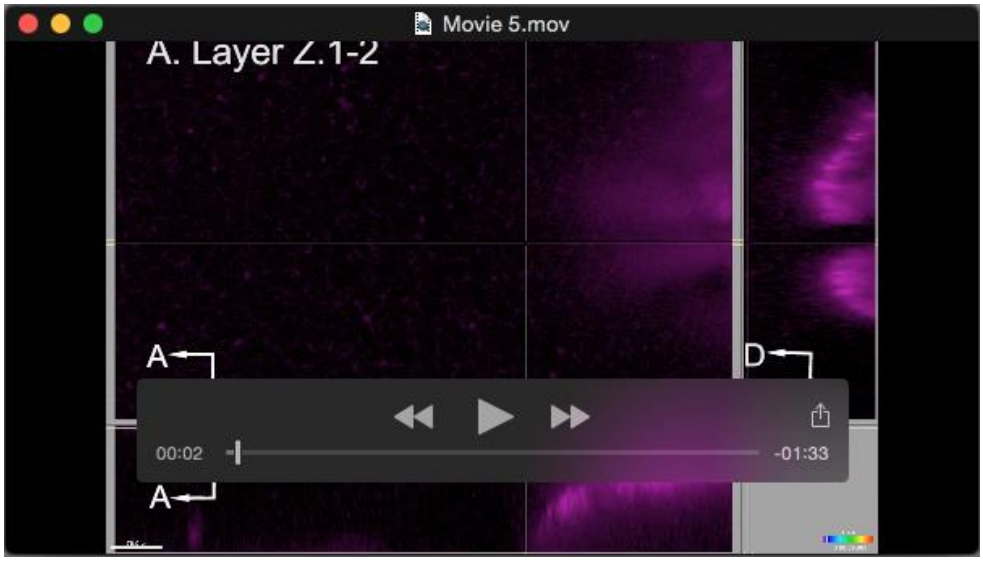

Movie 5. 4D imaging of distinct cell behaviors in different z layers during head formation.

Movie 5 derives from Movie 4; the image set has been cropped initially in the *xy* dimensions and later in the *z* dimension in order to direct the attention of the reader and to reduce computational time.

(A) Initial Z.1 movie segment focuses on proliferating non-neural ectoderm (NNE) are obvious throughout the z1 layer movie and are highlighted by a cyan circle.

(B) The Z.1 movie segment then transitions into a higher magnification view.

(C) Z.3-7 movie segment shows z3-7 layers and focuses on NC cells delaminating (denoted by cyan arrows) from the NT and migrating ventrolaterally beneath and along the NNE.

(D) Z.3-7 movie segment transitions into a higher magnification view.

(E) The Z.14 movie segment focuses on the NT as it moves anterior and presses against the anterior most NNE cells. The anterior end of the NT then flattens and bifurcates laterally as highlighted by black arrows. The head mesenchyme (M) is also apparent. The Z.14 movie segment then repeats without arrows (The Z.14 movie segment was fluorescently enhanced using Imaris and color inverted to view the deeper and thus dimmer cells.)

Dorsal view. Lower left scale bar: 200 um; grid scale marked every 200 um along xy axes; time scale in lower right corner; A, anterior; NT, neural tube; NC, neural crest. Arrows indicate how the various slices are oriented for anterior (A), lateral (L), and dorsal (D) directions. Microscope metadata same as Movie 4.

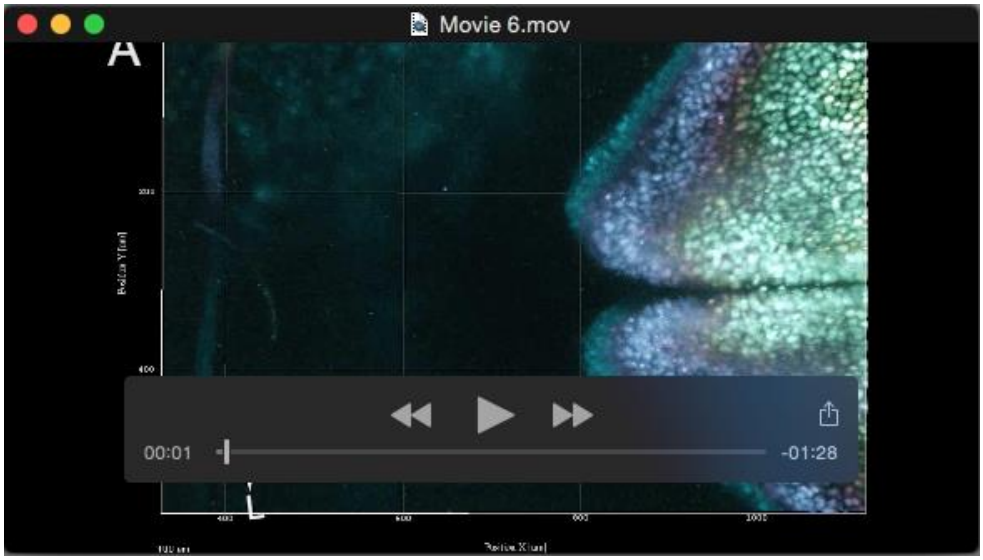

Movie 6. Color-coding of z layers helps visualize relative cell movements during head formation.

(A) To better visualize the relative movements chFP+ cells of cells and tissues in distinct z layers, we have color coded the image set with z1-2 in yellow, z3-7 in cyan, and z10-14 in magenta. Due to the curved structure of the dorsal head region, some NC cells are pseudo colored yellow and some ectoderm cells are pseudo colored cyan.

(B) NC cell egression (marked by cyan arrows) from the NT and bilateral migration are readily apparent with the ventral NT seen as a backdrop.

(C) Tracked cells are marked by an orange 'dragon tail' help visualize the speed and direction of individual cell movements overlay cells in Movie 6B.

(D) Tracked cells are marked by an orange 'dragon tail' help visualize the speed and direction of individual cell movements overlay cells in Movie 6A.

(E) 300% zoom of Movie 6D with focus on NC migration. Black circles surround putative yellow ectoderm cells to highlight the differences on cell movements within the distinct z layers. Cyan colored NC cells can be seen migrating beneath yellow ectoderm cells.

Dorsal view. Lower left scale bar: 200 um; grid scale marked every 200 um along xy axes; time scale in lower right corner; A, anterior; NT, neural tube; NC, neural crest. Lower left arrows indicate embryo is oriented for anterior (A) and lateral (L) directions.

Microscope metadata: Zeiss 510 META inverted, 20X/0.8 NA Plan-Apochromat; Ex 488 nm (12%)/Em BP 505-550; Ex 561 (15%)/Em LP 575.

Dimensions: 562.5 x 562.5 x 126 (21 z sections) μm^3; Voxel size: 2.2 x 2.2 x 6.0 μm^3; Bits per pixel: 8.

Acquisition time: Image montage (3 x 2 x 21), at 7:30 min intervals per *xyz* for a total of 29.5 hours was made by stitching *xyz* image sets across *t* with AIM LSM4.0 software.

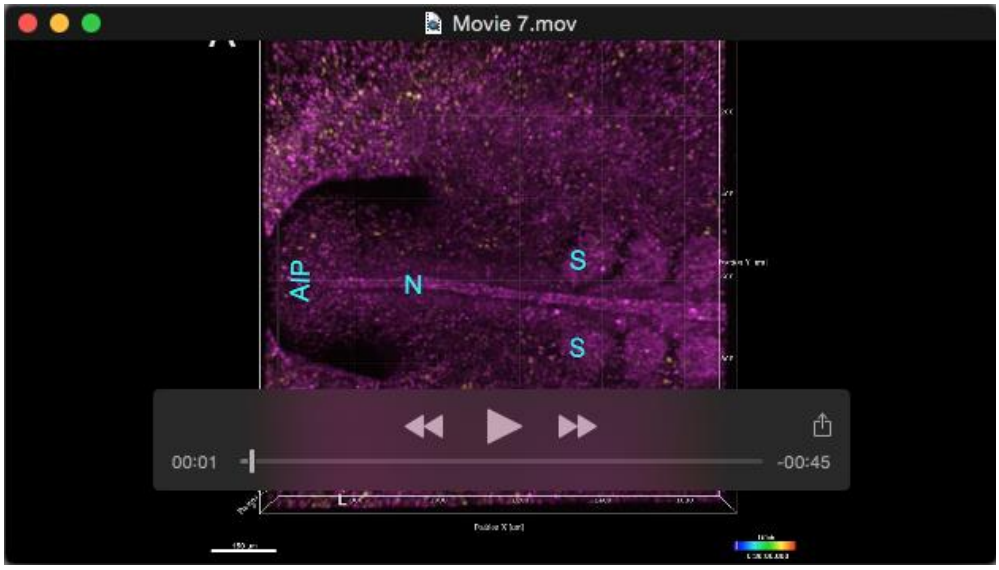

Movie 7. Multispectral 4D imaging of Tg(PGK1:H2B-chFP; TIE1:H2B-eYFP) embryo shows assembly of dorsal aortae in the context of the developing ventral trunk region.

Composite movie showing aorta formation in a Tg(PGK1:H2B-chFP; TIE1:H2B-eYFP) double transgenic quail embryo with all cell nuclei (magenta) and EC nuclei (yellow) concomitantly with descent of the AIP. Confocal microscopy of forming dorsal aortae from stages 8-11 (longitudinal view).

(A) The first movie segment shows an overlay of the image data for both the PGK1:H2B-chFP; TIE1:H2B-eYFP chFP+/YFP+ cells.

(B) Image data for only the chFP+ cells.

(C) Image data for only the YFP+ ECs. Angioblasts proliferate and migrate to positions of the presumptive DA in the embryo where they integrate primary vascular plexus. The embryo is oriented with the anterior end (A) on the left. Movie corresponds with data in Fig.5A-C.

Ventral view. Lower left scale bar: 150 um; grid scales mark every 200 um along xy axes; time scale in lower right corner; TIE1:H2B-eYFP+ ECs are pseudo-colored yellow; PGK1:H2B-chFP+ cells are pseudo-colored magenta; AIP, anterior intestinal portal; N, notochord; S, somite; DA, dorsal aorta. Lower left 3D arrows indicate that the embryo is oriented with anterior (A) to the left, lateral (L) to the bottom, and dorsal (D) into the page. Microscope metadata same as Movie 6.

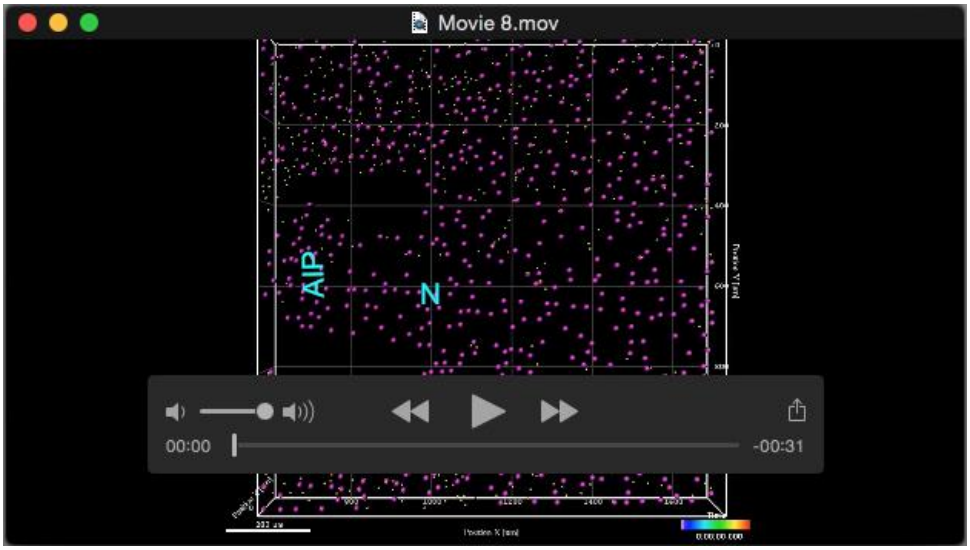

Movie 8. Multispectral 4D cell tracking (*xyzt*) of Tg(PGK1:H2B-chFP) trunk region with focus on dorsal aortae formation.

This movie shows cell-tracking analysis from the image set used to generate Movie 6 and Fig.5. The movie initially shows an overlay of the cell tracking data for both the PGK1:H2B-chFP; TIE1:H2B-eYFP chFP+/YFP+ cells, which is followed by the cell tracking data for only the chFP+ cells, which is followed by the cell tracking data for only the YFP+ ECs. The embryo is oriented with the anterior end (A) on the left. Movie corresponds to data in Fig.5D.

Ventral view. Lower left scale bar: 150 um; grid scales mark every 200 um along xy axes; time scale in lower right corner; TIE1:H2B-eYFP+ ECs are pseudo-colored yellow; PGK1:H2B-chFP+ cells are pseudo-colored magenta; AIP, anterior intestinal portal; N, notochord; DA, dorsal aortae. Lower right 3D arrows indicate that the embryo is oriented with anterior (A) to the left, lateral (L) to the bottom, and dorsal (D) into the page. Microscope metadata same as Movie 6.

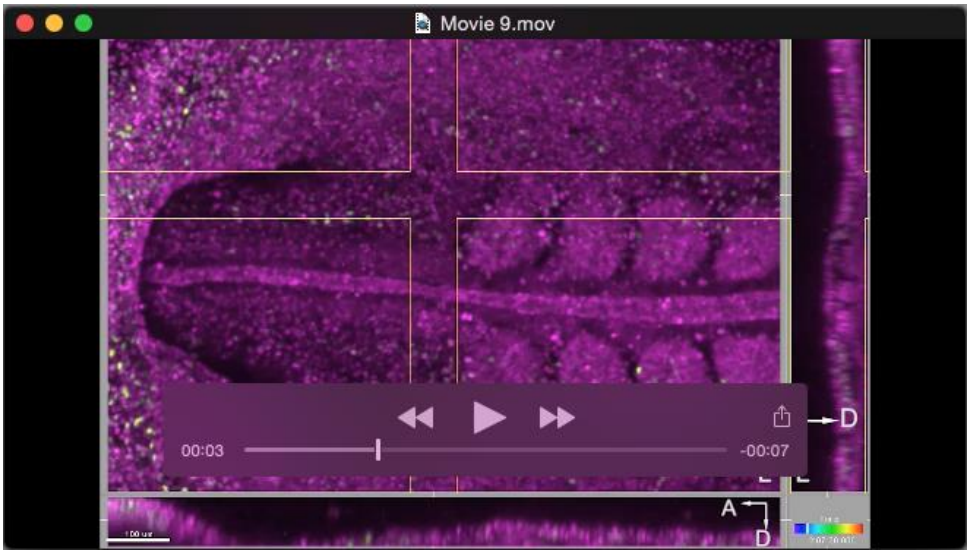

Movie 9. Dorsal aortae formation in 4D.

Confocal microscopy of forming dorsal aortae from stage 8-11 (longitudinal view). The embryo is oriented with the anterior end (A) on the left. This movie shows dorsal aorta formation in 4D from the image set used to generate Movie 6 and Fig.5.

Ventral view. Lower left scale bar: 100 um; time scale in lower right corner; TIE1:H2B-eYFP+ ECs are pseudo-colored yellow; PGK1:H2B-chFP+ cells are pseudo-colored magenta. AIP, anterior intestinal portal; N, notochord; S, somite; DA, dorsal aortae. Arrows indicate how the various slices are oriented for anterior (A), lateral (L), and dorsal (D) directions. Microscope metadata same as Movie 6.

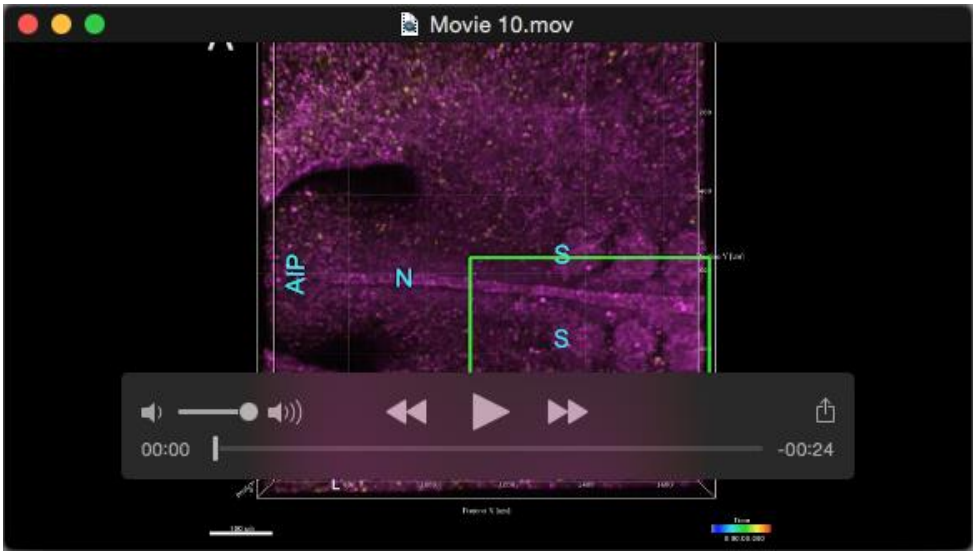

Movie 10. Dorsal aorta formation involves distinct cell behaviors.

A) The green box highlights and defines a higher magnification observation of aorta formation that focuses on EC proliferation, specification, migration and assembly. Putative angioblasts ($chFP^+YFP^-$) can be seen differentiating into ECs ($chFP^+YFP^+$) throughout the movie.

B) Cyan circles surround dividing progenitor cells ($chFP^+YFP^-$), while yellow circles surround representative ROIs of dividing H2B-eYFP+ ECs ($chFP^+YFP^+$) during the first 3 hrs of the movie. Numerous other cell divisions can be seen throughout the movie. The encircled cells quickly move beyond the perimeter of the circles as they collectively move with other embryonic cells during elongation along the A-P axis. Of note are putative angioblasts and ECs within the forming aorta; some of the cells appear to move anterior with the majority of their neighboring aortic cells and thus the general motion of the aorta, whereas other aortic cells continue to move randomly or in a posterior direction, but not anterior.

C) Other tissue specific cells tend to move similar to other cells within their affiliated tissue types as can be viewed within the green oblong: the notochord and adjacent somatic and aortic cells move steadily anterior while a ventral monolayer of putative endoderm cells (marked by white arrow) remain relatively static in terms of A-P motion but not individual motion. Note very bright chFP+ cell near point of arrow at time point 04:30:00 moves anterior at ~100 um/hr, similar to the notochord, somites, dorsal aorta, and adjacent tissue, while the presumptive endoderm cells (7-10 $chFP^+$ cells) remain near the fixed blue arrow.

Ventral view. Lower left scale bar: 70 um; grid scales mark every 200 um along *xy* axes; time scale in lower right corner; TIE1:H2B-$eYFP^+$ ECs are pseudo-colored yellow; PGK1:H2B-$chFP^+$ cells are pseudo-colored magenta; AIP, anterior intestinal portal; N, notochord; S, somite; DA, dorsal aorta. The movie has been slowed down 50%. Lower left 3D arrows indicate that the embryo is oriented with anterior (A) to the left, lateral (L) to the bottom, and dorsal (D) into the page. Microscope metadata same as Movie 6.

References

Chapman, S., Collignon, J., Schoenwolf, G. C. and Lumsden, A. (2001). Improved method for chick whole-embryo culture using a filter paper carrier. *Developmental Dynamics* **220**, 284-289.

Czirok, A., Rupp, P. A., Rongish, B. J. and Little, C. D. (2002). Multi-field 3D scanning light microscopy of early embryogenesis. *J Microsc* **206**, 209-217.

Drake, C. J., Davis, L. A. and Little, C. D. (1992). Antibodies to beta 1-integrins cause alterations of aortic vasculogenesis, in vivo. *Dev Dyn* **193**, 83-91.

Germroth, P. G., Gourdie, R. G. and Thompson, R. P. (1995). Confocal microscopy of thick sections from acrylamide gel embedded embryos. *Microsc Res Tech* **30**, 513-520.

New, D. (1955). A new technique for the cultivation of the chick embryo in vitro. *J Embryol Exp Morphol* **3**, 320-331.

Sato, Y., Poynter, G., Huss, D., Filla, M. B., Czirok, A., Choi, J. M., Rongish, B. J., Little, C. D., Fraser, S. E. and Lansford, R. (2010). Dynamic analysis of vascular morphogenesis using transgenic quail embryos. *PLoS ONE* **5**, e12674.

Warren, M., Puskarczyk, K. and Chapman, S. C. (2009). Chick embryo proliferation studies using EdU labeling. *Dev Dyn* **238**, 944-949.